SYNTHESIS, CRYSTAL STRUCTURES AND ELECTROCHEMISTRY OF FERROCENYL-SUBSTITUTED 1,3,4-OXADIAZOLES

Jiří TAUCHMAN[1], Jakub TRNKA[2], Ivana CÍSAŘOVÁ[3] and Petr ŠTĚPNIČKA[4],*

Charles University in Prague, Faculty of Science, Department of Inorganic Chemistry, Hlavova 2030, 128 40 Prague 2, Czech Republic; e-mail: [1] jira.t@centrum.cz, [2] jaktrn@seznam.cz, [3] cisarova@natur.cuni.cz, [4] stepnic@natur.cuni.cz

Dedicated to Dr. Bohumil Štíbr on the occasion of his 70th birthday.

Two ferrocenyl-substituted 1,3,4-oxadiazoles, 2-ferrocenyl-1,3,4-oxadiazole (**1**) and 2,5-diferrocenyl-1,3,4-oxadiazole (**2**), have been prepared from the corresponding hydrazides, (ferrocenecarbonyl)hydrazine (**3**) and 1,2-bis(ferrocenecarbonyl)hydrazine (**4**), and characterized by conventional spectroscopic methods (IR, NMR, MS) and elemental analyses. The solid-state structures of **1**, **2** and **4** have been determined by single-crystal X-ray diffraction analysis. The redox behavior of **1** and **2** was studied by electrochemical methods. Compound **1** underwent a reversible one-electron oxidation attributed to the ferrocene/ferrocenium couple ($E^{\circ\prime}$ = +0.28 V vs ferrocene/ferrocenium). On the other hand, compound **2** showed two closely separated anodic waves corresponding to two consecutive redox changes, indicating some degree of electronic communication between the ferrocenyl moieties in positions 2 and 5 at the 1,3,4-oxadiazole ring.
Keywords: Ferrocene; Heterocycles; 1,3,4-Oxadiazoles; Electrochemistry; Crystal structure.

Substituted 1,3,4-oxadiazoles have found various applications as biologically active compounds and building blocks for materials chemistry[1]. Despite their frequent use in the latter field, there is only little known about the redox-active, ferrocenyl-modified 1,3,4-oxadiazoles. Indeed, the archetypal compounds, 2-ferrocenyl-1,3,4-oxadiazole (**1**) (ref.[2]) and 2,5-diferrocenyl-1,3,4-oxadiazole (**2**) (ref.[3]) have already been reported. The former compound was obtained by the conventional condensation of ferrocenecarbohydrazide, $FcCONHNH_2$ (**3**; Fc = ferrocenyl), with triethyl orthoformate, whereas the diferrocenylated compound **2** and some related compounds, including the unsymmetric derivative (Ph/Fc), were obtained by $POCl_3$-mediated cyclization of the respective 1,2-diacylhydrazines,

FcCONHNHCOR (R = Fc or Ph) at elevated temperatures. The only other, recent examples we are aware of include the synthesis and an electrochemical polymerization study of 2-aminoaryl-5-ferrocenyl-1,3,4-oxadiazoles[4], and the preparation of some 4-ferrocenylphenyl-1,3,4-oxadiazole derivatives[5]. The lack of recent information concerning the ferrocene-modified 1,3,4-oxadiazoles and, particularly, unknown electrochemical properties of the basic representatives that are closely related to potential material applications led us to synthesize compounds **1** and **2**, and study their properties by a combination of structural and electrochemical methods.

RESULTS AND DISCUSSION

Syntheses and Characterization

Compound **1** was prepared (Scheme 1) by the general method based on the condensation/cyclization reaction of acylhydrazines with orthoesters[1a–1c,6]. Nonetheless, changing the reaction conditions (temperature and time) resulted in a cleaner and better yielding reaction as compared with the original procedure[2] (83 vs 43% isolated yield). Also, the intermediate ethoxymethylene hydrazide, FcCONHN=CHOEt, noted in previous experiments, was not isolated in the present case.
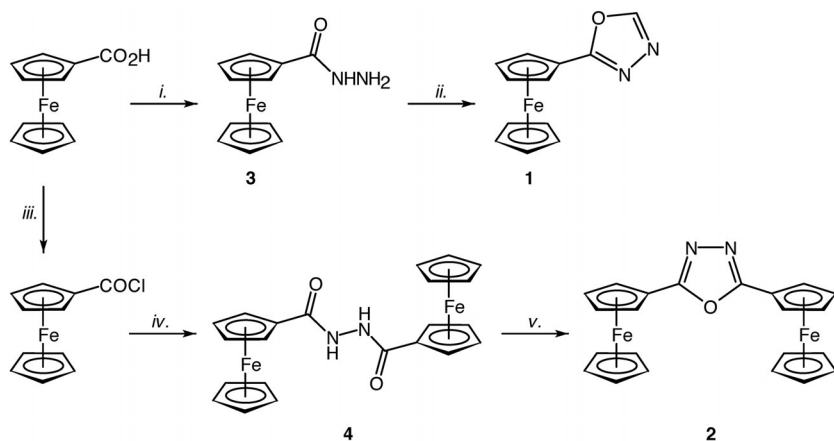
SCHEME 1

Preparation of ferrocenylated 1,3,4-oxadiazoles **1** and **2**: *i*. (1) excess diazomethane (THF/diethyl ether), (2) $N_2H_4 \cdot H_2O$ (methanol/refluxing; ref.[7]); *ii*. $HC(OEt)_3$/refluxing; *iii*. $(COCl)_2$ (dichloromethane/0 °C → room temperature; ref.[8]); *iv*. $N_2H_4 \cdot H_2O$ (pyridine/0 °C → room temperature); *v*. 2-chloro-1,3-dimethylimidazolinium chloride/triethylamine (dichloromethane/0 °C → room temperature)

The bis-ferrocenylated oxadiazole **2** was synthesized in two steps, starting from chlorocarbonylferrocene which was first treated with hydrazine hydrate in pyridine to afford 1,2-bis(ferrocenecarbonyl)hydrazine (**4**) in a 50% yield. Subsequent ring closure was effected by 2-chloro-1,3-dimethylimidazolinium chloride. This reagent was chosen mainly because it efficiently promotes ring closure of 1,2-diacyl hydrazines to 1,3,4-oxadiazoles[9] under mild conditions and, thus, the use of hazardous reagents (such as $SOCl_2$, $POCl_3$, CCl_3CN or $ZrCl_4$), high-boiling solvents (*N,N*-dimethylformamide, hexamethylfosforamide, etc.) and harsh reaction conditions (typically high temperatures) can be avoided[1a–1c]. Indeed, the reaction of **4** with 2-chloro-1,3-dimethylimidazolinium chloride in the presence of triethylamine (in dichloromethane, at room temperature for 40 h) followed by aqueous work-up and isolation by column chromatography afforded the desired heterocycle **2** in a good purity and 76% isolated yield.

Compounds **1**, **2** and **4** were characterized by their melting points, elemental analyses (conventional or from high-resolution mass spectra), and by NMR, MS and IR spectroscopies. In addition, the solid-state structures of **1**, **2** and **4** have been determined by single-crystal X-ray crystallography. Compounds **1** and **2** were also studied by electrochemical methods (vide infra).

The ^1H NMR spectrum of **1** displays a typical low-field signal of the single proton at the oxadiazole ring (δ_H 8.37) and signals due to the ferrocenyl unit: a sharp singlet of the C_5H_5 ring (δ_H 4.18) and two virtual triplets (δ_H 4.49 and 4.96) due to the AA'BB' spin system constituted by the C_5H_4 protons. Similarly, the $^{13}C\{^1H\}$ NMR spectrum of **1** combines the signals attributable to the ferrocenyl moiety and its oxadiazolyl substitutent. Resonances of the protonated and *ipso*-carbons within the oxadiazole ring are seen at δ_C 151.85 and 167.19, respectively. The ^1H NMR spectrum of **2** is very simple, showing only a set of characteristic signals due to the equivalent ferrocenyl groups at positions nearly identical to those observed for **1**. A similar description applies to the ^{13}C NMR spectrum, where an additional resonance of the equivalent C_{ipso} carbons in the oxadiazole ring is seen at δ_C 165.96.

IR spectra of the oxadiazoles display strong bands attributable to C=N stretching vibrations at 1589/1519 cm^{-1} for **1** and at 1599/1575 cm^{-1} for **2** [1b]. Both compounds further show a ν(CH) band of ferrocene CH groups at ca. 3085 cm^{-1}, while the spectrum of compound **1** features an additional sharp ν(CH) band at 3143 cm^{-1}, which can tentatively be attributed to the CH group in the oxadiazole ring. Other bands of the ferrocenyl moieties are found at expected positions (ca. 1000/1100, 820 and 480–500 cm^{-1})[10], and

can not be simply distinguished from other bands due to the heterocyclic ring.

Oxadiazoles **1** and **2** are thermally robust, showing highly abundant molecular ions in their electron-ionization mass spectra (base peaks for both compounds). The molecular ions decompose by elimination of HCN or HCNO from **1**$^{•+}$, and by elimination of FcCN or FcCNO from **2**$^{•+}$ to form ions isobaric with FcCNO$^{•+}$ (m/z 227) and FcCN$^{•+}$ (m/z 211), which corresponds with the fragmentation patterns observed for aryl-substituted 1,3,4-oxadiazoles[11]. In contrast, the acyl fragments (FcCO$^+$), typically encountered in the mass spectra of aryl 1,3,4-oxadiazoles, are insignificantly populated. The spectra further exhibit very distinct signals due to ferrocene fragments at m/z 121 ($C_5H_5Fe^+$) and 56 (Fe$^+$) but only poorly abundant ions possibly attributable to Fc$^+$ (m/z 185).

Crystal Structures

Compound **1** crystallizes in an orthorhombic crystal system with chiral space group $P2_12_12_1$ and one molecule per the asymmetric unit. A view of the molecular structure is presented in Fig. 1 along with selected interatomic distances and angles. The geometry of the oxadiazole moiety sug-
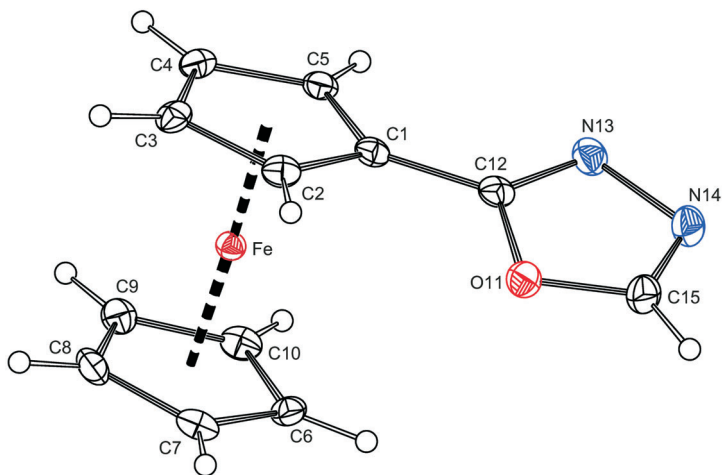

FIG. 1
PLATON[17] plot of the molecular structure of **1** showing the atom labelling scheme and displacement ellipsoids at 30% probability level. Selected distances (in Å) and angles (in °): C1–C12 1.447(3), C12–O11 1.369(2), C12–N13 1.294(3), N13–N14 1.422(3), N14–C15 1.277(3), C15–O11 1.352(3); C12–O11–C15 101.9(2), O11–C12–N13 112.5(2), C12–N13–N14 105.9(2), N13–N14–C15 105.3(2), N14–C15–O11 114.4(2)

gests a localized bond character and compares very well with that reported earlier for 2-methyl-5-phenyl-1,3,4-oxadiazole[12] and for symmetrically disubstituted compounds such as 2,5-diphenyl- (ref.[13]), 2,5-bis(4-tolyl)-(ref.[14]), 2,5-bis(4-cyanophenyl)- (ref.[15]) and 2,5-bis[4-(methoxycarbonyl)-phenyl]-1,3,4-oxadiazole[16].

Atoms forming the oxadiazole ring in **1** are almost perfectly coplanar (maximum deviation from the mean plane being 0.002 Å). However, the ring plane is rotated by 16.9(1)° with respect to its bonding cyclopentadienyl ring so that the oxygen atom O11 appears below the cyclopentadienyl plane, closer to the iron atom. The ferrocene moiety is quite regular, showing a negligible variation in the Fe–C distances (2.039(2)–2.056(2) Å). Accordingly, the tilt angle of the mean cyclopentadienyl planes is only 2.2(1)° and the Fe–Cg distances are rather similar (cf. 1.6495(9) and 1.654(1) Å for the substituted and non-substituted ring, respectively).

In the crystal, the individual molecules of **1** associate into infinite chains via soft hydrogen bonding interactions (Fig. 2) between the ferrocene H5 and the heterocyclic O11 in molecules associated by elemental translation along the crystallographic *a*-axis. The hydrogen bond parameters are as fol-
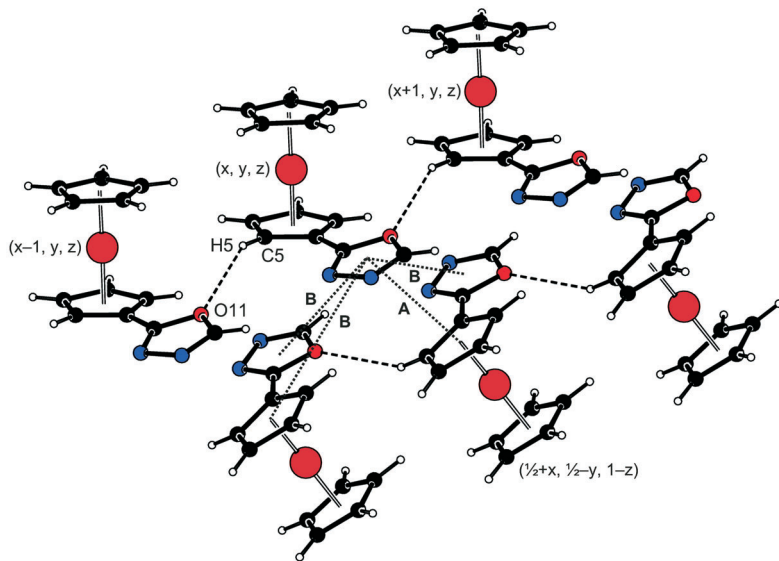

Fɪɢ. 2

A section of the molecular array in the crystal of **1** demonstrating the formation of infinite hydrogen-bonded chains and their mutual interactions. The hydrogen bonds are indicated with dashed lines. Possible interactions of the π-rings are highlighted with dotted lines connecting the respective ring centroids

lows: C5···O11 = 3.412(3) Å, H5···O11 = 2.59 Å, angle at H5 = 147°. Besides, the proximal chains related by the screw axis operations associate in a pairwise manner via π···π stacking interactions of the substituted cyclopentadienyl and the oxadiazole rings (interaction A in Fig. 2). The distance of the respective ring centroids is 3.678(1) Å and the rings are mutually tilted at the dihedral angle of the mean ring planes of 18.8(1)°. Other possible contacts (B in Fig. 2) are geometrically unfavorable, showing the distances of the ring centroids of ca. 5.27 Å. It is likely that the π-interactions (i.e., crystal packing effects) make the crystal assembly chiral by favoring a certain, non-coplanar orientation of the oxadiazole unit and its bonding cyclopentadienyl ring which, in turn, leads to axial chirality in the solid state. Additional stabilization of the molecular assembly comes from C–H···π-ring contacts between the ferrocene C8–H8 and the unsubstituted cyclopentadienyl ring in a molecule related by the (2 − x, 1/2 + y, 3/2 − z) symmetry operation (not shown in Fig. 2; C8···ring centroid = 3.822(2) Å, angle at H8 = 159°).

A view of the molecular structure of **2** is presented in Fig. 3 together with relevant interatomic distances and angles. Geometric parameters of the C_2N_2O ring are unexceptional in view of the data observed for **1** and the
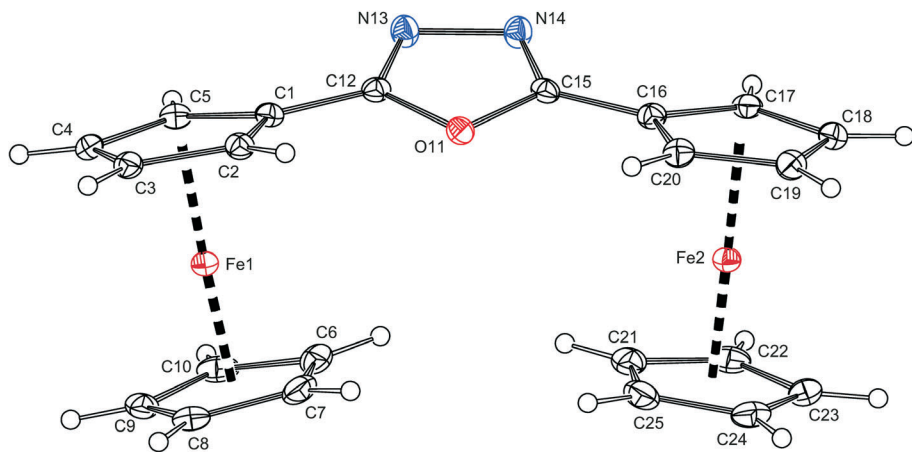

FIG. 3
PLATON plot of the molecular structure of **2** showing displacement ellipsoids at the 30% probability level. Selected distances (in Å) and angles (in °): C1–C12 1.450(2), O11–C12 1.367(2), C12–N13 1.291(2), N13–N14 1.422(2), N14–C15 1.294(2), C15–O11 1.366(2), C15–C16 1.453(2); C12–O11–C15 102.2(1), O11–C12–N13 113.1(2), C12–N13–N14 105.9(1), N13–N14–C15 105.8(1), N14–C15–O11 113.1(2)

reference compounds mentioned above. The arrangement of the central oxadiazole ring is almost perfectly symmetric: the ring atoms are coplanar within 0.003 Å, while the differences in the distances and angles 'related' by a virtual plane that is perpendicular to the ring plane and passes atom O11 and the midpoint of the N13–N14 bond, are as low as 0.001 Å and 0.1°, respectively. Also, the ferrocenyl groups attached in positions 2 and 5 are both directed to one side of the oxadiazole ring. Yet, they assume slightly different orientations towards the oxadizole ring, which ultimately lowers the overall molecular symmetry. The dihedral angles subtended by the oxadiazole plane and the planes of the substituted cyclopentadienyl rings are 24.7(1) and 19.0(1)° for the ferrocenyl groups involving Fe1 and Fe2, respectively. Otherwise, however, the ferrocenyl substitutents adopt regular geometries, showing only marginal variation in the Fe–C bond lengths (2.036(2)–2.060(2) Å for Fe1, 2.036(2)–2.056(2) Å for Fe2) and insignificant tilting (the dihedral angles of the least-squares cyclopentadienyl planes are 3.6(1)° (Fe1) and 2.1(2)° (Fe2)). The distances from Fe1 to the cyclopentadienyl ring centroids are 1.6507(8) Å for the substituted and 1.657(1) Å for the unsubstituted ring. The same parameters involving the second ferrocenyl group (Fe2) are 1.6485(9) and 1.653(1) Å.

The crystal structure of **2** is essentially molecular, showing neither C–H···X (X = O or N) contacts nor extensive π-stacking interactions of the aromatic rings. For instance, the most favorable π···π interaction is detected for the unsubstituted cyclopentadienyl ring bonding to Fe1 and its inversion-related image with the distance of the ring centroids being ca. 4.05 Å and ring slippage of ca. 2.33 Å (N.B. the interacting rings are exactly parallel due to their symmetry relation). The only other intermolecular interactions worth mentioning (Fig. 4) are the pairs of C–H···π-ring contacts formed between the CH groups of the substituted cyclopentadienyl rings located in positions adjacent to the oxadiazole nitrogen atoms and π-systems of the same cyclopentadienyl rings in a molecule related by the crystallographic 2_1 screw axis (1/2 – x, 1/2 + y, 1/2 – z). Parameters of these interactions are as follows: C5–H5···Cg(B), C5···Cg(B) = 3.569(2) Å, angle at H5 = 172°; C17–H17···Cg(A), C17···Cg(A) = 3.790(2) Å, angle at H17 = 160° (Cg(A) and Cg(B) stands for the centroids of the rings C(1-5) and C(16-20), respectively).

Due to crystal defects and poor diffraction ability of the available crystals, the structure determination of **4** is of a relatively low precision (see Experimental). Hence, the discussion will be restricted only to important molecular parameters and, mainly, to the crystal packing. The compound crystallizes with five molecules in the centrosymmetric triclinic unit cell (space

group *P*-1). Whereas two crystallographically independent molecules are found in general positions (molecules **2** and **3**), the last one completing the asymmetric unit by its half is located around the crystallographic inversion centre (molecule **1**).
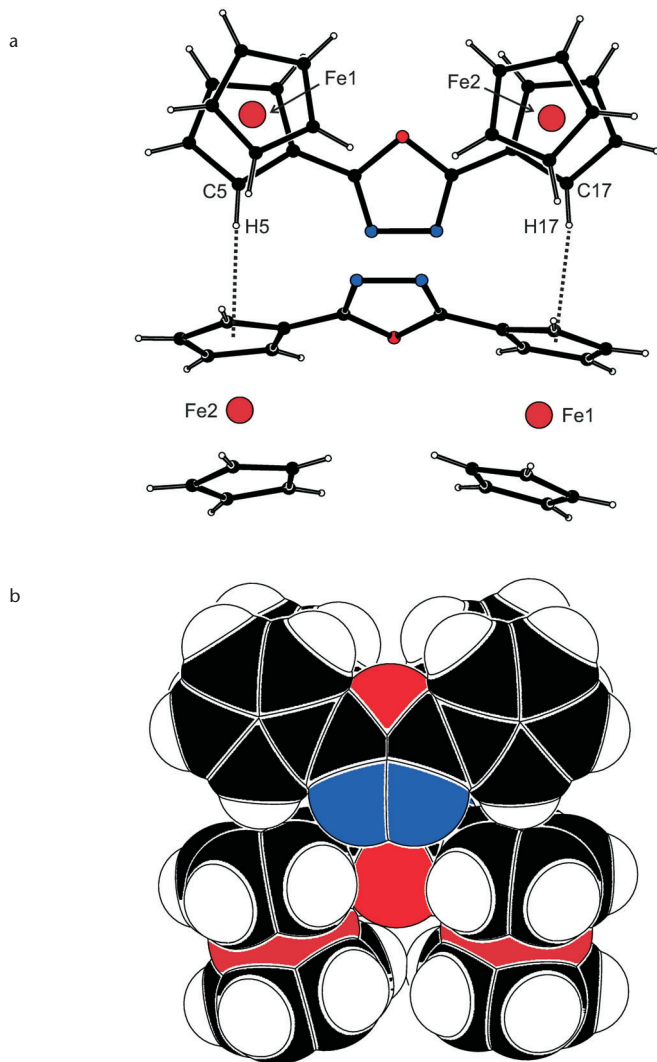

<small>Fig. 4</small>
Ball-and-stick (a) and space-filling (b) representations of the dimeric unit encountered in the crystal of **2**. The C–H⋯π-ring interactions are indicated with dotted lines in part a

Views of the independent molecules are shown in Fig. 5. The selected geometric data for all molecules are summarized in Table I. The molecular geometries are unexceptional, particularly in view of the data reported earlier for **3** (ref.[7b]) and for PhCONHNHCOPh [18] as an organic analogue. How-
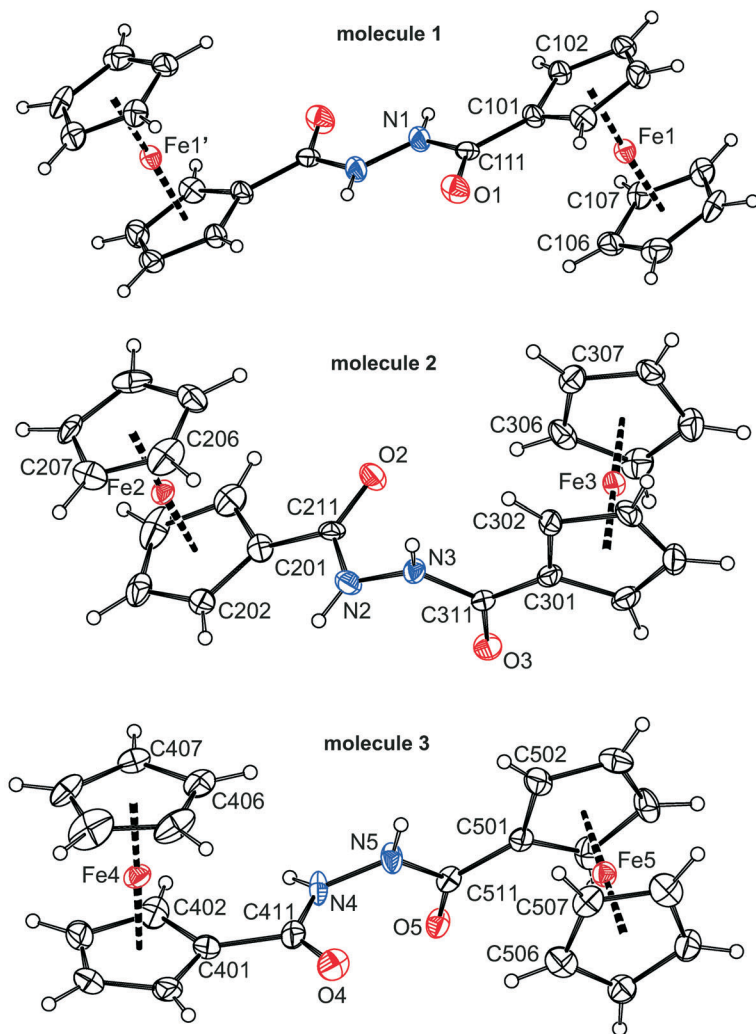

Fig. 5

PLATON plots of the crystallographically independent molecules of hydrazide **4** showing atom labelling scheme and displacement ellipsoids at the 30% probability level. Mutual orientation of the molecules does not correspond with that encountered in the crystal

TABLE I
Comparison of the geometric parameters for the structurally independent molecules of **4**[a]

Parameter	Molecule 1[d]	Molecule 2[f]	Molecule 3[f]
C=O	1.22(2)	1.21(2)/1.24(2)	1.22(2)/1.24(2)
C–N	1.37(2)	1.38(2)/1.38(2)	1.34(2)/1.35(2)
O=C–N	121(1)	123(1)/122(1)	125(1)/122(1)
N–N	1.39(2)	1.39(2)	1.39(2)
τ[b]	180[e]	88(1)	111(2)
∠Cp1,Cp2	3.5(9)	4.2(9)/4.0(9)	2(1)/5.8(9)
φ[c]	8(2)	8(2)/1(2)	6(2)/7(2)
Fe–Cg1	1.637(7)	1.652(7)/1.638(6)	1.632(9)/1.646(7)
Fe–Cg2	1.644(7)	1.647(7)/1.653(7)	1.635(8)/1.651(7)

[a] Definitions: Cp1 = substituted cyclopentadienyl ring, Cp2 = unsubstituted cyclopentadienyl ring; Cg1 and Cg2 are the respective centroids. [b] Torsion angle at the N–N bond (C–N–N–C). [c] Dihedral angle subtended by the carbamoyl {CON} moiety and its parent Cp1 ring. [d] Single values due to the imposed symmetry. [e] This value reflects the imposed symmetry. [f] Values for the part with lower atomic numbers are given first.
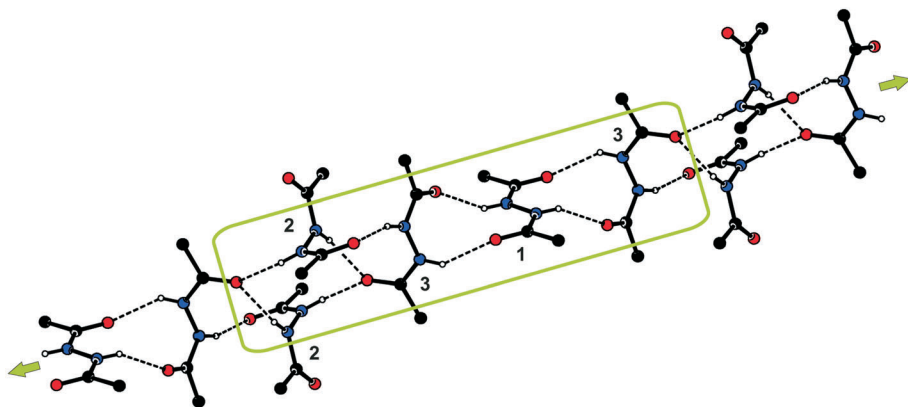

FIG. 6
Section of the hydrogen-bonded array in the crystal of **4**. For clarity, only the pivotal carbon atoms (Cn11, n = 1 – 5) from each ferrocenyl group and amide hydrogens are shown. The 'independent' part of the molecular assembly is highlighted with a green box while the arrows indicate where the propagation occurs. The numbers are used to denote the structurally independent molecules

ever, the individual molecules differ markedly in the overall conformation, namely by the orientation of the acyl groups attached to the NH–NH moiety and by the mutual rotation of the ferrocenyl groups. Thus, in molecule 1, the acyl groups as well as the ferrocenyl pendants assume *anti* positions due the imposed symmetry. In molecules 2 and 3, on the other hand, they are rotated at the C–N–N–C torsion angles being ca. 88 and 111°, which corresponds to an intermediate conformation between synclinal and anticlinal in the former case and to an anticlinal conformation in the latter. The O···O distances are 4.70(2) Å for molecule 1, 3.65(1) Å for molecule 2, and 4.03(1) Å for molecule 3.

Individual molecules in the crystal of **4** associate predominantly[19] by means of N–H···O=C hydrogen bonds, forming twisted ribbons in the direction of the crystallographic *c*-axis (Fig. 6). The repeating unit of the hydrogen-bonded array is constituted by molecule 1 which acts as a hydrogen-bond donor and a hydrogen-bond acceptor for each of two adjacent molecules 3 mutually related by crystallographic inversion. Molecules 3 further bind (again as both H-bond donor and acceptor) to a pair involving molecule 2 and its inversion-related image. The number of molecules involved in the repeating H-bonded unit thus corresponds with the number of molecules being crystallographically independent (1 + 2 × 2). It should be noted that the five structurally unique O···N distances fall into a rather narrow range of 2.84(2)–2.94(1) Å.

Electrochemistry

Oxadiazoles **1** and **2** have been studied by cyclic voltammetry (Fig. 7), differential pulse voltammetry at a stationary platinum disc electrode (Fig. 8) and by voltammetry at a rotating disc electrode, using 1 mM solutions in 1,2-dichloroethane containing 0.1 M Bu_4NPF_6 as the supporting electrolyte. In cyclic voltammetry, compound **1** showed a standard reversible one-electron wave with peak currents and peak-to-peak separation very similar to those of ferrocene under identical conditions. This redox process can be attributed to ferrocene-based oxidation affording the corresponding ferrocenium, and occurs at +0.28 V vs the ferrocene/ferrocenium reference, in agreement with an expected electron-withdrawing nature of the 1,3,4-oxadiazol-2-yl moiety. The reversible, one-electron character was confirmed by voltammetry at rotating disc electrode, during which compound **1** exhibited a standard sigmoidal wave with limiting current very similar to that of ferrocene at the same concentration and measurement conditions.

In contrast, the redox response of **2** was more complicated as the compound underwent two closely spaced one-electron oxidations (Fig. 7). The anodic and cathodic maxima in cyclic voltammetry were found at ca. +0.33 and +0.13 V vs ferrocene/ferrocenium (at 200 mV s^{-1} scan rate). The presence of two consecutive redox steps was indicated also by differential pulse voltammetry that showed a broad unresolved peak apparently resulting from convolution of two insufficiently separated peaks (Fig. 8). During conventional voltammetry at a rotating disc electrode, the compound dis-
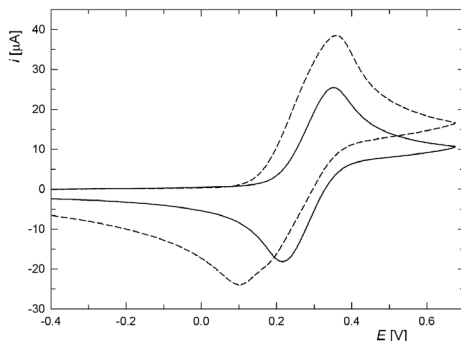
Fig. 7
Cyclic voltammograms of **1** (full line) and **2** (dashed line) as recorded in 1,2-dichloroethane at a platinum disc electrode and 200 mV s^{-1} scan rate. The potentials are given relative to the standard ferrocene/ferrocenium couple
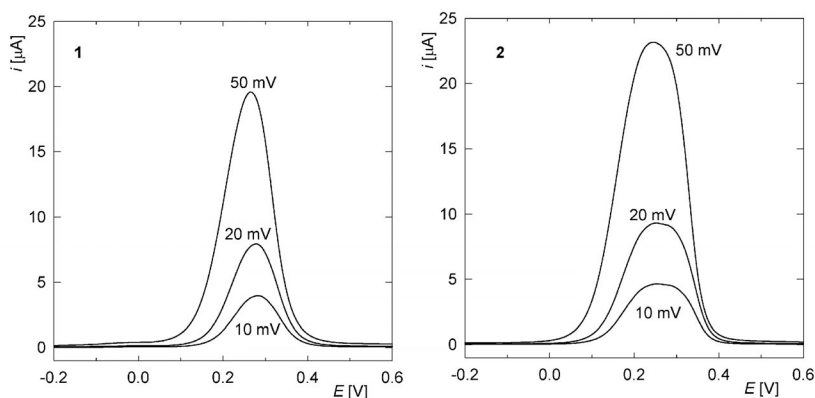
Fig. 8
Differential pulse voltammograms of **1** (left) and **2** (right) recorded with different modulation amplitudes (given in the graphs). The potentials are given relative to the standard ferrocene/ferrocenium couple

played an anodic wave with a maximum, which suggests some chemical complications to be associated with the primary electron-transfer reactions.

CONCLUSION

In summary, we have prepared ferrocenyl- and 2,5-diferrocenyl-1,3,4-oxadizoles from the respective ferrocencarbonyl hydrazines either by using a slightly modified original procedure or with the aid of a recently introduced cyclization reagent. The compounds have been characterized by their melting points, combustion analyses and conventional spectroscopic methods (NMR, IR, MS). Their solid-state structures have been determined by X-ray diffraction analysis. Electrochemical methods have shown that the mono-ferrocenylated compound undergoes one-electron reversible oxidation, most likely localized at the ferrocene moiety. Oxidation of the 2,5-diferrocenyl derivative proceeds as two closely separated redox steps, pointing to some degree of electronic communication between the ferrocenyl units.

EXPERIMENTAL

Materials and Methods

All syntheses were carried out under an argon atmosphere in the dark. (Ferrocenecarbonyl)-hydrazine (**3**) (ref.[7]) and chlorocarbonylferrocene[8] were prepared according to literature procedures. Anhydrous dichloromethane was purchased from Fluka. Pyridine was distilled from potassium hydroxide under argon. Other chemicals (Fluka, Aldrich) and solvents (Penta) were used as received from commercial sources.

NMR spectra were measured with a Varian UNITY Inova 400 spectrometer at 25 °C. Chemical shifts (δ, ppm) are given relative to internal tetramethylsilane ($\delta_H = \delta_C = 0$ ppm). Coupling constants J are given in Hz. IR spectra (v_{max}, cm^{-1}) were recorded from Nujol mulls on an FT IR Nicolet Magna 650 spectrometer. Electron-ionization (EI) mass spectra were recorded with a GCT Premier spectrometer (Waters). Electrospray-ionization (ESI) mass spectra including the high-resolution (HR) measurements were obtained with an LCQ Fleet spectrometer (Thermo Fisher Scientific). Melting points were determined on a Kofler block.

Electrochemical measurements were performed with a multipurpose potentiostat µAUTOLAB III (Eco Chemie, Netherlands) at room temperature, using a standard three-electrode cell equipped with a platinum disc working electrode (AUTOLAB RDE, 3 mm diameter), a platinum sheet auxiliary electrode, and a saturated calomel reference electrode (SCE) that was separated from the analysed solution by a salt-bridge (0.1 M Bu$_4$NPF$_6$ in 1,2-dichloroethane). The analysed compounds were dissolved in dry 1,2-dichloroethane (Sigma–Aldrich) to give a solution containing 1 mM analysed compounds and 0.1 M Bu$_4$NPF$_6$ (Fluka, purissimum for electrochemistry) as the supporting electrolyte. The solutions were deaerated by bubbling with argon before the measurement and then kept under an argon blanket. The redox potentials are given relative to the ferrocene/ferrocenium reference.

Preparation of 2-Ferrocenyl-1,3,4-oxadiazole (**1**)

(Ferrocenecarbonyl)hydrazine (122 mg, 0.50 mmol) was mixed with triethyl orthoformate (5 ml, 30 mmol) and the resulting suspension was sonicated in an ultrasonic bath for 5 min. Then, the reaction vessel was equipped with a reflux condenser, flushed with argon and heated at 140 °C (the temperature in the bath) for 18 h. After this time, the mixture was cooled to room temperature and the volatiles were removed under vacuum. The residue was dissolved in dichloromethane (5 ml) and the solution was evaporated again. The crude reaction product was purified by column chromatography on silica gel eluting with dichloromethane–methanol (20:1 v/v). The single band which developed was collected and evaporated under vacuum to afford essentially pure **1** as an orange-brown solid. Yield 105 mg (83%). M.p. 123–125 °C (heptane; lit.[2] gives 120–122 °C). ^1H NMR (CDCl$_3$): 4.18 s, 5 H (C$_5$H$_5$); 4.49 virtual t, J' = 2.0 Hz, 2 H (C$_5$H$_4$); 4.96 virtual t, J' = 2.0, 2 H (C$_5$H$_4$); 8.37 s, 1 H (C$_2$HON$_2$). $^{13}C\{^1H\}$ NMR (CDCl$_3$): 65.96 s (C$_{ipso}$ of C$_5$H$_4$); 68.19 s (CH of C$_5$H$_4$); 69.89 s (C$_5$H$_5$); 70.95 s (CH of C$_5$H$_4$); 151.85 s (CH of C$_2$HON$_2$); 167.19 s (C$_{ipso}$ of C$_2$HON$_2$). IR (Nujol): ν(CH) aromatic 3143 (m) and 3085 (w); ν(C=N) 1589 (s) and 1519 (m); 1306 (m), 1240 (m), 1118 (m), 1106 (m), 1087 (s), 1036 (m), 1023 (m), 967 (m), 953 (m), 946 (w), 881 (w), 848 (w), 840 (w), 821 (m), 736 (s), 637 (s), 619 (w), 518 (s), 509 (s), 487 (s), 445 (w). EI+ MS, m/z (relative abundance): 255 (14), 254 (100, M$^+$), 252 (8), 227 (18, [M – HCN]$^+$), 212 (4), 211 (27, [M – HCNO]$^+$), 199 (10), 198 (10, probably [M – N$_2$ – CO]$^+$), 184 (4), 172 (12), 133 (12), 128 (4), 121 (31, [C$_5$H$_5$Fe]$^+$), 115 (4), 98 (3), 95 (4), 94 (4), 81 (5), 56 (30, Fe$^+$). For C$_{12}$H$_{10}$FeN$_2$O (254.07) calculated: 56.72% C, 3.97% H, 11.03% N; found: 56.39% C, 3.91% H, 10.64% N. Note: Analytical sample was crystallized from hot heptane.

Preparation of 1,2-Bis(ferrocenecarbonyl)hydrazine (**4**)

A solution of chlorocarbonylferrocene (519 mg, 2.1 mmol) in dry pyridine (3 ml) was added to a mixture of hydrazine hydrate (48 μl, 1.0 mmol) and pyridine (5 ml) while cooling on ice. The cooling bath was removed and the resulting mixture was stirred at room temperature overnight, and then evaporated under vacuum. The solid residue was partitioned between ethyl acetate and 5% aqueous KOH. The organic layer was separated, washed with brine, dried over MgSO$_4$ and evaporated with chromatographic silica gel. The pre-adsorbed material was transferred onto a top of a chromatographic column (silica gel; ethyl acetate–hexane 1:1 v/v) and the column was eluted first with ethyl acetate–hexane (1:1 v/v) and then with ethyl acetate. The product eluted slowly in a yellow band, which was evaporated to give **4** as a yellow-orange solid. Yield 226 mg (50%). ^1H NMR ((CD$_3$)$_2$SO): 4.34 s, 5 H (C$_5$H$_5$); 4.41 virtual t, J' = 1.9, 2 H (C$_5$H$_4$); 4.89 virtual t, J' = 1.9, 2 H (C$_5$H$_4$); 9.56 s, 1 H (NH). $^{13}C\{^1H\}$ NMR ((CD$_3$)$_2$SO): 68.20 s (CH of C$_5$H$_4$); 69.58 s (C$_5$H$_5$); 70.10 s (CH of C$_5$H$_4$); 74.10 s (C$_{ipso}$ of C$_5$H$_4$); 168.82 s (C=O). ESI MS: 457 [M + H]$^+$, 479 [M + Na]$^+$, 455 [M – H]$^-$. HR ESI MS calculated for C$_{22}$H$_{21}$Fe$_2$N$_2$O$_2$ 457.0302 ([M + H]$^+$), found 457.0296.

Preparation of 2,5-Diferrocenyl-1,3,4-oxadiazole (**2**)

1,2-Bis(ferrocenecarbonyl)hydrazine **4** (137 mg, 0.30 mmol) was mixed with dry dichloromethane. The resulting suspension was cooled and treated successively with dry triethylamine (0.1 ml, ca. 0.7 mmol) and 2-chloro-1,3-dimethylimidazolinium chloride (56 mg, 0.33 mmol) dissolved in dichloromethane (3 ml). The reaction mixture was stirred at room temperature for 40 h, whereupon the solid hydrazide gradually dissolved to give a brown so-

lution. The reaction solution was washed with 5% aqueous citric acid, saturated aqueous sodium hydrogencarbonate and brine, dried over $MgSO_4$ and evaporated under vacuum. The solid residue was purified by chromatography on a short silica gel column using methanol–dichloromethane (1:20 v/v) as an eluent. Subsequent evaporation afforded compound **2** as an orange solid. Yield 99 mg (76%). M.p. 224–226 °C (ethyl acetate–hexane; lit.[3] gives 222–224 °C). ^{1}H NMR (CDCl$_3$): 4.21 s, 5 H (C$_5$H$_5$); 4.49 virtual t, J' = 1.9, 2 H (C$_5$H$_4$); 4.99 virtual t, J' = 1.9, 2 H (C$_5$H$_4$). ^{13}C{^{1}H} NMR (CDCl$_3$): 66.89 s (C$_{ipso}$ of C$_5$H$_4$); 67.96 s (CH of C$_5$H$_4$); 69.83 s (C$_5$H$_5$); 70.68 s (CH of C$_5$H$_4$); 165.96 s (C$_{ipso}$ of C$_2$HON$_2$). IR (Nujol): ν(CH) aromatic 3084 (w); 1648 (w); ν(C=N) 1599 (s) and 1575 (s); 1271 (w), 1139 (w), 1105 (s), 1037 (m), 1031 (m), 999 (m), 965 (m), 881 (m), 823 (s), 745 (m), 513 (vs), 485 (m), 441 (w) cm^{-1}. EI+ MS, m/z (relative abundance): 439 (20), 438 (100, M$^+$), 436 (11), 346 (4), 320 (5), 268 (5), 227 (12, [M – FcCN]$^+$), 213 (6), 211 (20, [M – FcCNO]$^+$), 186 (4), 185 (7, Fc$^+$), 172 (4), 133 (7), 129 (7), 121 (22, [C$_5$H$_5$Fe]$^+$), 56 (10, Fe$^+$). For C$_{22}$H$_{18}$Fe$_2$N$_2$O·0.1C$_7$H$_{16}$ (448.10) calculated: 60.84% C, 4.41% H, 6.25% N; found: 60.84% C, 4.35% H, 6.22% N. Note: Analytical sample was crystallized from hot heptane.

X-ray Crystallography

Crystals suitable for single-crystal X-ray diffraction analysis were grown by crystallization from hot heptane (**1**: rusty orange bar, 0.08 × 0.10 × 0.53 mm^3), ethyl acetate–hexane (**2**: orange prism, 0.05 × 0.10 × 0.28 mm^3) or from hot (ca. 80%) aqueous acetic acid (**4**: orange plate, 0.15 × 0.20 × 0.58 mm^3). The selected specimens were mounted on glass fibres with poly(perfluoroalkyl ether) oil (ABCR). Full-set diffraction data (±h,±k,±l; θ ≤ 27.5° for **1** and **2**, θ ≤ 25.5° for **4**; data completeness ≥ 99%) were collected with a Nonius KappaCCD diffractometer equipped with a Cryostream Cooler (Oxford Cryosystems). The measurements were performed in a stream of dry nitrogen at 150(2) K, using graphite-monochromatized MoKα radiation (λ = 0.71073 Å). The data for **2** were corrected for absorption using a gaussian integration method based on the indexed crystal shape as included in the diffractometer software.

The structures were solved by direct methods (SIR97[20]) and refined by full-matrix least squares on F^2 (SHELXL97[21]). The non-hydrogen atoms were refined with anisotropic displacement parameters while the hydrogens were included in their calculated positions and refined as riding atoms with U_{iso}(H) assigned to 1.2U_{eq} of their bonding carbon atom. Compound **4** crystallized in the form of plate-like blocks composed from rather loosely connected sheets, which resulted in crystal defects and, hence, in a decrease in the coherent diffraction volume and poor diffraction properties. Besides, the diffraction data showed signs of non-merohedral twinning, which was accounted for by PLATON program[17]. The twin components were found to be related by the twin law (–1.000, 0.000, 0.000/0.189, 1.000, 0.201/0.000, 0.000, –1.000) and their contributions refined to ca. 36:64. No absorption correction was made. The relatively poor quality of the diffraction data and crystal defects is reflected in the relatively low overall precision and high values of the final R-indices and the residual electron density. However, the overall chemical picture is unambiguous.

Relevant crystallographic data are given in Table II. Geometric parameters and structural drawings were obtained with a recent version of the PLATON program[17]. All calculated values are rounded with respect to their estimated standard deviations (esd's) given with one digit; parameters involving atoms in constrained positions are given without esd's.

Compound	1	2	4
Formula	$C_{12}H_{10}FeN_2O$	$C_{22}H_{18}Fe_2N_2O$	$C_{22}H_{20}Fe_2N_2O_2$
M, g mol^{-1}	254.07	438.08	456.10
Crystal system	orthorhombic	monoclinic	triclinic
Space group	$P2_12_12_1$ (no. 19)	$P2_1/n$ (no. 14)	P-1 (no. 2)
a, Å	5.7356(2)	10.8462(2)	11.3294(3)
b, Å	7.4278(2)	7.4562(2)	12.3333(5)
c, Å	23.6562(6)	21.5206(5)	17.0223(6)
deg			96.931(2)
deg		95.880(2)	102.019(2)
deg			93.312(2)
V, Å^3	1007.82(5)	1731.24(7)	2300.9(1)
Z	4	4	5
D_{calc}, g dm^{-3}	1.674	1.681	1.646
MoKα, mm^{-1}	1.471	1.690[e]	1.597
Diffractions total	11665	31132	41653
R_{int}, %[b]	4.1	6.1	7.4
Unique diffractions	2319	3964	8419
Observed[c] diffractions	1998	3022	6627
Number of parameters	145	244	632
Flack's enantiomorph parameters	–0.01(2)	n.a.	n.a.
R (observed diffractions), %[c,d]	2.46	2.89	11.4
R, wR (all diffractions), %[d]	3.39, 5.44	4.62, 7.59	13.5, 29.3
Δ, e Å^{-3}	0.40, –0.33	0.49, –0.43	1.42, –1.19
CCDC entry	778839	778840	778841

[a] Common details: T = 150(2) K. [b] $R_{int} = \Sigma|F_o^2 - F_o^2(\text{mean})|/\Sigma F_o^2$, where $F_o^2(\text{mean})$ is the average intensity of symmetry-equivalent diffractions. [c] Diffractions with $I_o > 2\sigma(I_o)$. [d] $R = \Sigma||F_o| - F_c||/\Sigma|F_o|$, $wR = [\Sigma\{w(F_o^2 - F_c^2)_2\}/\Sigma\ w(F_o^2)^2]^{1/2}$. [e] Absorption correction was applied; range of transmission coefficients 0.639–0.906.

CCDC 778839 (**1**), 778840 (**2**) and 778841 (**4**) contain the supplementary crystallographic data for this paper. These data can be obtained free of charge via www.ccdc.cam.ac.uk/conts/retrieving.html (or from the Cambridge Crystallographic Data Centre, 12, Union Road, Cambridge, CB2 1EZ, UK; fax: +44 1223 336033; or deposit@ccdc.cam.ac.uk).

REFERENCES AND NOTES

1. a) Nesynov E. P., Grekov A. P.: *Usp. Khim.* **1964**, *33*, 1184 (English version: *Russ. Chem. Rev.* **1964**, *33*, 508); b) Hetzheim A., Möckel K.: *Adv. Heterocycl. Chem.* **1967**, *7*, 183; c) Jakopin Ž., Sollner Dolenc M.: *Curr. Org. Chem.* **2008**, *12*, 850; d) Krasovitskii B. M., Bolotin B. M.: *Organic Luminiscent Materials*. Wiley-VCH, Weinheim 1988.
2. Popp F. D., Moynahan E. B.: *J. Heterocycl. Chem.* **1970**, *7*, 739.
3. Lorkowski H.-J., Pannier R., Wende A.: *J. Prakt. Chem.* **1967**, *35*, 149.
4. Chiang C. C., Chen H.-C., Lee C., Leung M., Lin K.-R., Hsieh K.-H.: *Chem. Mater.* **2008**, *20*, 540.
5. Sarhan A. A. O., Izumi T.: *J. Organomet. Chem.* **2003**, *675*, 1.
6. Ainsworth C.: *J. Am. Chem. Soc.* **1955**, *77*, 1148.
7. a) Osgerby J. M., Pauson P. L.: *J. Chem. Soc.* **1961**, 4604; b) Štěpnička P., Císařová I., Nižňanský D., Bakardjieva S.: *Polyhedron* **2010**, *29*, 134.
8. Kojima T., Noguchi D., Nakayama T., Inagaki Y., Shiota Y., Yoshizawa K., Ohkubo K., Fukuzumi S.: *Inorg. Chem.* **2008**, *47*, 886.
9. Isobe T., Ishikawa T.: *J. Org. Chem.* **1999**, *64*, 6989.
10. Nakamoto K.: *Infrared and Raman Spectra of Inorganic and Coordination Compounds*, 5th ed., Part B, Chap. IV-6, p. 285. Wiley, New York 1997.
11. Belenkii L. I., Luiksaar S. I., Poddubnyi I. S., Krayushkin M. M.: *Izv. Akad. Nauk SSSR, Ser. Khim.* **1998**, 2309 (English version: *Russ. Chem. Bull.* **1998**, *47*, 2238); and references therein.
12. Emmerling F., Reck G., Kraus W., Orgzall I., Schulz B.: *Cryst. Res. Technol.* **2008**, *43*, 99 (structure determined from X-ray powder diffraction data).
13. Kuzentsov V. P., Patsenker L. D., Lokshin A. I., Tolmachev A. V.: *Funct. Mater.* **1996**, *3*, 460.
14. a) Reck G., Orgzall I., Schulz B.: *Acta Crystallogr., Sect. E: Struct. Rep. Online* **2003**, *59*, o1135; b) The geometric parameters were calculated from the data deposited with the Cambridge Crystallographic Data Centre (refcode: OJIFES).
15. a) Dong Y.-B., Wang H.-Y., Ma J.-P., Shen D.-Z., Huang R.-Q.: *Inorg. Chem.* **2005**, *44*, 4679; b) The geometric parameters were calculated from the data deposited with the Cambridge Crystallographic Data Centre (refcode: LARMIB).
16. a) Reck G., Orgzall I., Schulz B., Dietzel B.: *Acta Crystallogr., Sect. C: Cryst. Struct. Commun.* **2003**, *59*, o634; b) The geometric parameters were calculated from the data deposited with the Cambridge Crystallographic Data Centre (refcodes: BEBMAX and BEMAX01; two polymorphs).

17. a) Spek A. L.: *J. Appl. Crystallogr.* **2003**, *36*, 7; b) The program is available via the Internet at http://www.cryst.chem.uu.nl/platon/.
18. Shanmuga Sundara Raj S., Yamin B. M., Boshaala A. M. A., Tarafder M. T. H., Crouse K. A., Fun H.-K.: *Acta Crystallogr., Sect. C: Cryst. Struct. Commun.* **2000**, *56*, 1011.
19. Some intermolecular C–H···O contacts are also detected.
20. Altomare A., Burla M. C., Camalli M., Cascarano G. L., Giacovazzo C., Guagliardi A., Moliterni A. G. G., Polidori G., Spagna R.: *J. Appl. Crystallogr.* **1999**, *32*, 115.
21. Sheldrick G. M: *SHELXL97, Program for Crystal Structure Refinement from Diffraction Data.* University of Göttingen, Göttingen 1997.